The pseudo 2-D relaxation model for obtaining T_1–T_2 relationships from 1-D T_1 and T_2 measurements of fluid in porous media

Nathan H. Williamson[a,*], Magnus Röding[b,c], Huabing Liu[d,e], Petrik Galvosas[d], Stanley J. Miklavcic[f], Magnus Nydén[a,c]

[a] Future Industries Institute, University of South Australia, Mawson Lakes, SA 5095, Australia.
[b] SP Agrifood and Bioscience, Frans Perssons väg 6, 402 29 Göteborg, Sweden.
[c] School of Energy and Resources, UCL Australia, University College London, 220 Victoria Square, Adelaide, SA 5000, Australia.
[d] MacDiarmid Institute for Advanced Materials and Nanotechnology, School of Chemical and Physical Sciences, Victoria University of Wellington, PO Box 600, Wellington, New Zealand.
[e] Limecho Technology Limited Company, Beijing 102299, China
[f] Phenomics and Bioinformatics Research Centre, School of Information Technology and Mathematical Sciences, University of South Australia, Mawson Lakes, SA 5095, Australia

Abstract

NMR spin-lattice (T_1) and spin-spin (T_2) relaxation times and their inter-relation possess information on fluid behaviour in porous media. To elicit this information we utilise the pseudo 2-D relaxation model (P2DRM), which deduces the T_1–T_2 functional relationship from independent 1-D T_1 and T_2 measurements. Through model simulations we show empirically that the P2DRM accurately estimates T_1–T_2 relationships even when the marginal distributions of the true joint T_1–T_2 distribution are unknown or cannot be modeled. Estimates of the T_1:T_2 ratio for fluid interacting with pore surfaces remain robust when the P2DRM is applied to simulations of rapidly acquired data. Therefore, the P2DRM can be useful in situations where experimental time is limited.

Keywords:
Relaxation correlation; Lognormal distribution; Inverse-gamma distribution; Magnetic resonance in porous media; Heterogeneity; Multidimensional distribution function

1. Introduction

Nuclear Magnetic Resonance (NMR) relaxation measurements provide a non-invasive means of studying fluid-saturated porous media. Heterogeneity of porous materials leads to distributions of spin-lattice (T_1) and spin-spin (T_2) relaxation times arising from the fluid within [1]. Since T_1 and T_2 are functions of the same material properties, e.g., surface-to-volume ratio [2], these quantities have a functional relationship [3]. The T_1–T_2 relationship provides information about surface interactions [4], which is unobtainable from a 1-D distribution alone. Venkataramanan et al. developed an efficient algorithm [5] for estimating a joint T_1–T_2 (probability) distribution from T_1–T_2 correlation experiment [6] data [3]. The T_1–T_2 distributions of porous media systems (e.g. fluid-saturated sandstones and carbonates [3]) confirm [7] that the observed relaxation rates often follow the Brownstein-Tarr [2] equations for the fast-diffusion limit, i.e., a sum of surface (ρ_1 or ρ_2) and bulk contributions, with the sum controlled by the surface-to-volume ratio:

$$\frac{1}{T_{1,2}} = \frac{1}{T_{1,2\ \mathrm{bulk}}} + \rho_{1,2}\frac{S}{V}. \tag{1}$$

From this pair a T_1–T_2 relationship can be described by a single monotonic equation [8]

$$\frac{1}{T_1} = K + \frac{\varepsilon}{T_2} \tag{2}$$

where $K = 1/T_{1\ \mathrm{bulk}} - \varepsilon/T_{2\ \mathrm{bulk}}$ and $\varepsilon = \rho_1/\rho_2$. If the T_1–T_2 relationship of a system follows Eq. (2) then it is obtainable from 1-D measurements. This was inferred as early as 1993 when Kleinberg et al. obtained single values of the T_1:T_2 ratio of rock cores by applying a cross-correlation function to the 1-D T_1 and T_2 distributions [9]. We developed the pseudo 2-D relaxation model (P2DRM): a method for obtaining T_1–T_2 distribution functions from 1-D T_1 and T_2 measurements [8]. The mathematical framework of relating distributions in this way was published by Röding et al. and is not specific to NMR [10]. The P2DRM is a 2-step parametric model fitting routine of independent 1-D T_1 and T_2 measurements. Parameter estimates from the T_2 data fit in the first step are used to constrain the T_1 data fit in the second step, making it possible to estimate the T_1–T_2 relationship without a 2-D data set. The utility of imposing constraints in multiple data fitting steps was also shown by Benjamini and Basser [11], who found that constraining the distribution fit of 2-D relaxation and diffusion data by the estimated marginal distributions from fits to 1-D data led to a significant reduction in the amount of data required for a stable fit. In the P2DRM, utilizing Eq. (2) as prior knowledge allows for the parameters K and ε to be fit directly in the second step. A pseudo 2-D T_1–T_2 distribution results from mapping the independent 1-D probability distributions to 2-D space using the assumed T_1–T_2 relationship.

In our previous publication [8], when tested on simulated data for fluid in rock, the pseudo 2-D distributions estimated by

*Corresponding author E-mail: nathan.williamson@mymail.unisa.edu.au

the P2DRM were consistent with the known joint T_1–T_2 distribution. However, in that case, the parametric models which the P2DRM used were good choices in that they were capable of describing the known joint T_1–T_2 distribution. Though we gave physical justification for the parametric model sets used, in practice one does not have prior knowledge of the appropriate model. The first point of this publication is to test whether the P2DRM can accurately estimate the T_1–T_2 relationship when the parametric model sets are incapable of describing the marginal distributions of the true joint T_1–T_2 distribution. Utilizing a rapid T_1 measurement along with the Carr-Purcell-Meiboom-Gill (CPMG) T_2 measurement potentially offers a means of estimating the T_1–T_2 relationship in situations where experimental time is limited such as for investigation of time-sensitive processes. The second point of this publication is to test the capability of the P2DRM to utilize rapidly acquired data in estimating the T_1–T_2 relationship.

The theory section includes equations for using lognormal or inverse-gamma distributions and their associated T_1 distributions as components in distribution models. Model sets are physically motivated and defined. The equations are reproduced from our previous publication [8] (and its corrigendum [12]). The methods section explains the data simulation and the fitting routine. Simulations give us access to the known joint T_1–T_2 distribution and allow us to test the limits of the P2DRM. The results and discussion section compares the pseudo 2-D distributions estimated by the P2DRM to the known joint T_1–T_2 distribution. We test the accuracy and precision by obtaining parameter estimates from 100 data simulations and fits.

2. Theory

The CPMG sequence [13, 14] measures the distribution of T_2 relaxation times, $f(T_2)$, by acquiring the signal from the center of each echo in a train of 180° RF pulses. The signal, $I(t_2)$, as a function of the acquisition time, t_2, is related to $f(T_2)$ by

$$I(t_2) = I_0 \int_0^\infty f(T_2) \exp(-t_2/T_2)\, dT_2, \tag{3}$$

where I_0 is the signal intensity at $t_2 = 0$. A class of rapid T_1 measurements built off the Look-Locker method [15] uses a series of short tip-angle RF pulses to linearly sample signal at tens to hundreds of points in the time domain with a single scan. In a double-shot implementation by Chandrasekera et al. [16], the signal from the FID following the n^{th} RF pulse of angle θ is

$$I\{(n-1)\tau_1\} = M_0 \sin\theta (\cos\theta)^{n-1} \int_0^\infty f(T_1)(\exp(-(n-1)\tau_1/T_1))dT_1 \tag{4}$$

where τ_1 is the time between RF pulses, the acquisition time is $t_1 = (n-1)\tau_1$, and M_0 is the initial magnetization. The signal intensity at $t_1 = 0$ is $I_0 = M_0 \sin\theta$.

A numerical inverse Laplace transform method is used to obtain $f(T_2)$ or $f(T_1)$. The result is a non-unique estimate of the actual relaxation time distribution and is dependent on the choice of model [17, 18]. Parametric models are based on physically motivated information and use a pre-defined number of components involving a commensurate number of pre-defined functions [18, 19, 20]. The P2DRM uses parametric models to allow for the utilization of Eq. (2) as prior knowledge. More specifically, for a given parametric distribution component of the $f(T_2)$ model, Eq. (2) can be used in a change-of-variables to define the parametric form of the component as a function of T_1. First, for the lognormal distribution of T_2,

$$P_{\mathrm{logN}}(T_2) = \frac{1}{\sigma T_2 \sqrt{2\pi}} \exp\left(-\frac{1}{2\sigma^2}(\ln T_2 - \mu)^2\right), \tag{5}$$

a change-of-variables using Eq. (2) results in

$$P_{\mathrm{BT\ logN}}(T_1) = \frac{1}{(1-KT_1)(\sigma T_1 \sqrt{2\pi})} \times \exp\left(-\frac{1}{2\sigma^2}(\ln\varepsilon + \ln T_1 - \ln(1-KT_1) - \mu)^2\right). \tag{6}$$

The subscript BT refers to Brownstein-Tarr. The parameters μ and σ control the shape of Eq. (5) and K and ε control the transformation of Eq. (5) to Eq. (6).

Second, for the inverse-gamma distribution of T_2,

$$P_{\Gamma^{-1}}(T_2) = \frac{\beta^\alpha}{\Gamma(\alpha)} T_2^{-\alpha-1} \exp\left(-\frac{\beta}{T_2}\right), \tag{7}$$

a change-of-variables using Eq. (2) results in

$$P_{\mathrm{BT}\ \Gamma^{-1}}(T_1) = \frac{\varepsilon}{(1-KT_1)^2} \frac{\beta^\alpha}{\Gamma(\alpha)} \left(\frac{\varepsilon T_1}{1-KT_1}\right)^{-\alpha-1} \times \exp\left(-\frac{\beta(1-KT_1)}{\varepsilon T_1}\right), \tag{8}$$

with parameters α and β equal to their value in Eq. (7) and again the only free parameters are K and ε.

Model sets must include a T_2 distribution model, $f(T_2)$, and an associated T_1 distribution model, $f(T_1)$. Model sets can utilize any combination of component functions, including delta functions so long as the two associated $P(T_2)$ and $P(T_1)$ functions come as pairs in attempting to represent the same population of spins. We use two model sets, 'model set A' and 'model set B' which each include a distribution plus delta function. Model set A incorporates $P_{\mathrm{logN}}(T_2)$ and $P_{\mathrm{BT\ logN}}(T_1)$ as the distributed component. The distributed component in model set B is represented by $P_{\Gamma^{-1}}(T_2)$ and $P_{\mathrm{BT}\ \Gamma^{-1}}(T_1)$. The fact that $T_1 \geq T_2$ is utilized to constrain the delta function. We have found model sets with a distributed component plus a delta function component to be more robust than model sets with a single distributed component and more stable than model sets with two distributed components. Inclusion of a delta function is physically motivated by the fact that as pore size increases, the Brownstein-Tarr fast diffusion limit will no longer apply and a significant portion of fluid in the interior of the pore can be described as having relaxation times equal to bulk values. Non-parametric, uniform-penalty inversions (UPEN) of relaxation experiments performed on porous media systems often show a sharp peak near the bulk relaxation time with a broad shoulder extending to short relaxation times [21], perhaps indicating that such a physical motivation is well-founded.

The pseudo 2-D T_1–T_2 distribution exists along the T_1–T_2 relationship described by Eq. (2) and the estimated values of K and ε. Due to the probability distribution being infinitely thin in all directions other than along the T_1–T_2 relationship, the function for the pseudo 2-D T_1–T_2 distribution is related to the 1-D marginal T_1 or T_2 distribution by a line integral. When parameterized by T_2, the resulting function is

$$P_c(T_2) = \frac{P(T_2)}{\sqrt{1 + \frac{\varepsilon^2}{(\varepsilon + K T_2)^4}}} \quad (9)$$

where $P(T_2)$ is the 1-D marginal T_2 distribution, either $P_{\mathrm{logN}}(T_2)$ or $P_{\Gamma^{-1}}(T_2)$. The subscript c refers to $P_c(T_2)$ being a distribution along a curve in T_1–T_2 space.

3. Methods

Paramagnetic species along pore walls determine surface relaxivities [1, 7]. Foley et al. measured T_1 and T_2 of water in packed calcium silicate powders synthesized with known concentrations of iron paramagnetic ions [22]. The iron concentration had a stronger effect on ρ_2 than ρ_1,

$$\rho_1 = 4.05\ \mu\text{m/s} + (0.000819\ \mu\text{m/s/ppm})[\text{Fe}]_{\text{ppm}}, \quad (10a)$$

$$\rho_2 = 3.96\ \mu\text{m/s} + (0.00227\ \mu\text{m/s/ppm})[\text{Fe}]_{\text{ppm}}, \quad (10b)$$

and therefore a distribution of iron concentrations can lead to a distribution of T_1–T_2 relationships. We simulated data sets by randomly sampling a large number of discrete radii and iron concentration values from a prescribed pore size and iron distribution, assigning T_1 and T_2 values to each radii and iron concentration pair using Eqs. (10) and Eqs. (1) and modeling signal relaxation as a sum of contributions from all radii and iron concentration pairs. The known joint T_1–T_2 distribution is a 2-D histogram from the discrete T_1 and T_2 values. The prescribed pore radii distribution was a sum of two lognormal distributions (the first with w = 0.8, mean = 27 μm, and standard deviation (std) = 36 μm, the second with mean = 380 μm and std = 200 μm), which creates a bimodal T_1–T_2 distribution. The prescribed paramagnetic iron distribution was lognormal with mean = 3.6×10^4 ppm and std = 4.8×10^4 ppm, similar to concentrations found in many sandstones and carbonates [22]. Through Eqs. (10) the iron distribution corresponded to a ρ_2/ρ_1 distribution with mean = 2.37 and std = 0.28. Bulk relaxation times were $T_{1\ \text{bulk}} = T_{2\ \text{bulk}}$ = 2 s. Discrete relaxation time values found using Eqs. (1) were used in Eqs. (3) and (4) to simulate CPMG data (with 4000 echoes and a 400 μs echo time) and rapid T_1 data (with 100 RF pulses of $\theta = 5°$ and τ_1 = 30 ms). The signal to noise ratio (SNR = $I_0/\sigma_{\text{noise}}$) was set to 340 for the T_2 data and 34 for the T_1 data by adding zero mean Gaussian noise.

The parametric distribution model sets A and B were employed in Eqs. (3) and (4) for a 2-step fitting of the 1-D data sets. The estimated values of K and ε complete the T_1–T_2 relationship described by Eq. (1). The pseudo 2-D T_1–T_2 distribution was determined from the results and Eq. (9). A least-squares fitting routine was implemented in MATLAB R2015a (Mathworks, Natick, USA) and was made available as supplementary material to ref. [8].

4. Results and discussion

The fits of distribution model sets A and B to simulated T_2 and T_1 relaxation data and the residuals of the fits are shown in Fig. 1. The factor $(\cos\theta)^{n-1}$ seen in Eq. (4) was divided from the T_1 signal intensity.

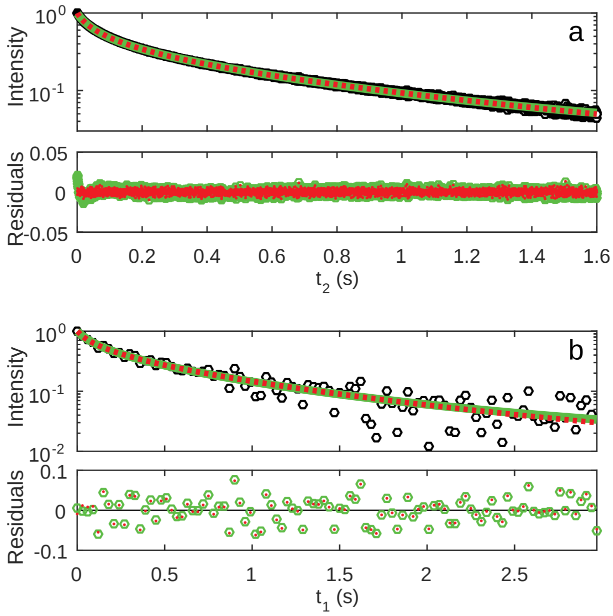

Figure 1: Results from using the P2DRM model sets A (red dotted line) and B (green solid line) to fit the simulated 1-D CPMG T_2 data (a) and rapid T_1 data (b), showing signal intensity (black circles), fits, and residuals.

The pseudo 2-D distributions estimated by the P2DRM are compared to the known joint 2-D distribution in Fig. 2. Both model sets estimated essentially the same T_1–T_2 relationship and both trace the known T_1–T_2 relationship. The delta functions are near the bulk relaxation limit, though inconsistent with one another and at T_1 values below the known T_1–T_2 relationship. The inability of the model sets to describe the marginal distributions of the known joint T_1–T_2 distribution results in the distributed components being shifted to shorter relaxation times. Even so, the models still show good agreement with the known T_1–T_2 relationship. With respect to fitting 1-D data, we have found parametric distribution models which under-fit the data, e.g., using a single distributed component to model the decay from a multimodal distribution, are still capable of estimating the means, $\langle T_2 \rangle$ or $\langle T_1 \rangle$. We can extend this to the P2DRM because obtaining the T_1–T_2 relationship in essence involves estimating the conditional $\langle T_1 \rangle$ given a value of T_2 (this is what the P2DRM T_1–T_2 relationship curve describes). For these reasons, P2DRM estimations of T_1–T_2 relationships are robust with respect to model assumptions.

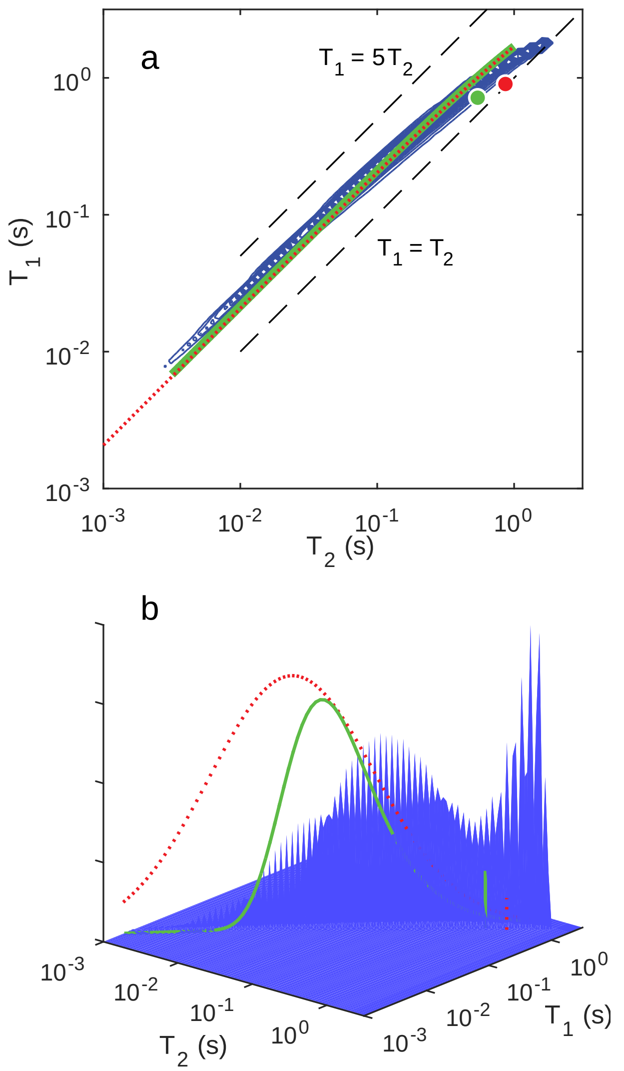

Figure 2: Results of the pseudo 2-D T_1–T_2 distributions from using P2DRM model sets A, based on the lognormal, (red dotted line) and B, based on the inverse-gamma, (green solid line) to fit the 1-D data sets compared to the known joint T_1–T_2 distribution (blue intensity map) highlighting (a) the T_1–T_2 relationships and (b) intensity of the distributions. The maximum intensities of the P2DRM distribution components are scaled by their weights.

Information about surface interactions can be gleaned from the ratio T_1:T_2 for fluid interacting with surfaces and ε^{-1} is therefore the key parameter for the P2DRM to obtain. From fitting 100 data sets simulated with unique instances of random noise, estimates of ε^{-1} for model set A (mean=2.54, std=0.43) and model set B (mean=2.41, std=0.43) were not significantly different from the known mean of the distribution of ρ_2/ρ_1 = 2.37. Data with this SNR could be acquired in a timescale of minutes, versus a timescale of hours for the T_1–T_2 correlation experiment. Therefore, the P2DRM should indeed be useful in situations where experimental time is limited.

Acknowledgements

This research was funded by the South Australian Government Premier's Research and Industry Grant project 'A Systems Approach to Surface Science', as well as the Australian Government International Presidents Scholarship (IPS).

References

[1] R. L. Kleinberg, W. E. Kenyon, P. P. Mitra, Mechanism of NMR relaxation of fluids in rock, J. Magn. Reson., Series A 108 (2) (1994) 206–214.

[2] K. R. Brownstein, C. E. Tarr, Importance of classical diffusion in NMR-studies of water in biological cells, Phys. Rev. A 19 (6) (1979) 2446–2453.

[3] Y. Q. Song, L. Venkataramanan, M. D. H urlimann, M. Flaum, P. Frulla, C. Straley, T_1-T_2 correlation spectra obtained using a fast two-dimensional laplace inversion, J. Magn. Reson. 154 (2) (2002) 261–268.

[4] P. J. McDonald, J. P. Korb, J. Mitchell, L. Monteilhet, Surface relaxation and chemical exchange in hydrating cement pastes: a two-dimensional NMR relaxation study, Phys. Rev. E 72 (1) (2005) 011409.

[5] L. Venkataramanan, Y.-Q. Song, M. D. Hrlimann, Solving Fredholm integrals of the first kind with tensor product structure in 2 and 2.5 dimensions, IEEE Trans. Signal. Process. 50 (5) (2002) 1017–1026.

[6] H. Peemoeller, R. K. Shenoy, M. M. Pintar, Two-dimensional NMR time evolution correlation spectroscopy in wet lysozyme, J. Magn. Reson. (1969) 45 (2) (1981) 193–204.

[7] S. Godefroy, J.-P. Korb, M. Fleury, R. G. Bryant, Surface nuclear magnetic relaxation and dynamics of water and oil in macroporous media, Phys. Rev. E 64 (2001) 021605–13.

[8] N. H. Williamson, M. Röding, P. Galvosas, S. J. Miklavcic, M. Nydén, Obtaining T_1–T_2 distribution functions from 1-dimensional T_1 and T_2 measurements: The pseudo 2-D relaxation model , J. Magn. Reson. 269 (2016) 186 – 195.

[9] R. L. Kleinberg, S. A. Farooqui, M. A. Horsfield, T_1/T_2 ratio and frequency dependence of NMR relaxation in porous sedimentary rocks, J. Colloid Interface Sci. 158 (1) (1993) 195–198.

[10] M. Röding, S. J. Bradley, N. H. Williamson, M. R. Dewi, T. Nann, M. Nydén, The power of heterogeneity: Parameter relationships from distributions, PLoS ONE 11 (5) (2016) e0155718.

[11] D. Benjamini, P. J. Basser, Use of marginal distributions constrained optimization (MADCO) for accelerated 2D MRI relaxometry and diffusometry, J. Magn. Reson. 271 (2016) 40 – 45.

[12] N. H. Williamson, M. Röding, P. Galvosas, S. J. Miklavcic, M. Nydén, Corrigendum to Obtaining T_1-T_2 distribution functions from 1-dimensional T_1 and T_2 measurements: The pseudo 2-D relaxation model [J. Magn. Reson. 269 (2016) 186195] , J. Magn. Reson. 271 (2016) 110.

[13] H. Y. Carr, E. M. Purcell, Effects of diffusion on free precession in nuclear magnetic resonance experiments, Phys. Rev. 94 (3) (1954) 630–638.

[14] S. Meiboom, D. Gill, Modified spin-echo method for measuring nuclear relaxation times, Rev. Sci. Instrum. 29 (8) (1958) 688–691.

[15] D. C. Look, D. R. Locker, Saving in measurement of NMR and epr relaxation times, Review of Scientific Instruments 41 (2) (1970) 250–251.

[16] T. C. Chandrasekera, J. Mitchell, E. J. Fordham, L. F. Gladden, M. L. Johns, Rapid encoding of T_1 with spectral resolution in n-dimensional relaxation correlations, J. Magn. Reson. 194 (1) (2008) 156–161.

[17] K. P. Whittall, A. L. MacKay, Quantitative interpretation of NMR relaxation data, J. Magn. Reson. 84 (1) (1989) 134–152.

[18] M. Röding, N. H. Williamson, M. Nydén, Gamma convolution models for self-diffusion coefficient distributions in PGSE NMR, J. Magn. Reson. 261 (2015) 6–10. doi:10.1016/j.jmr.2015.10.001.

[19] M. Röding, D. Bernin, J. Jonasson, A. Särkkä, D. Topgaard, M. Rudemo, M. Nydén, The gamma distribution model for pulsed-field gradient NMR studies of molecular-weight distributions of polymers, J. Magn. Reson. 222 (2012) 105–111.

[20] K. J. Layton, M. Morelande, D. Wright, P. M. Farrell, B. Moran, L. A. Johnston, Modelling and estimation of multicomponent T_2 distributions, IEEE Trans. Med. Imaging 32 (8) (2013) 1423–1434.

[21] G. Borgia, R. Brown, P. Fantazzini, Uniform-penalty inversion of multiexponential decay data, J. Magn. Reson. 132 (1) (1998) 65–77.

[22] I. Foley, S. Farooqui, R. Kleinberg, Effect of paramagnetic ions on NMR relaxation of fluids at solid surfaces, J. Magn. Reson., Series A 123 (1) (1996) 95–104.